Fletcher, David H.; Likongwe, Patrick J.; Chiotha, Sosten S.; Nduwayezu, Gilbert; Mallick, Dwijen; Uddin Md., Nasir; Rahman, Atiq; Golovátina-Mora, Polina; Lotero, Laura; Bricker, Stephanie; Tsirizeni, Mathews; Fitch, Alice; Panagi, Marios; Ruiz Villena, Cristina; Arnhardt, Christian; Vande Hey, Joshua; Gornall, Richard; Jones, Laurence. 2021. **Using demand mapping to assess the benefits of urban green and blue space in cities from four continents.**

The definitive version was published in *Science of the Total Environment*, 785, 147238. 12, pp. https://doi.org/10.1016/j.scitotenv.2021.147238

The definitive version is available at https://www.elsevier.com/

Title: Using demand mapping to assess the benefits of urban green and blue space in cities from four continents.

Abstract:

The benefits of urban green and blue infrastructure (UGI) are widely discussed, but rarely take into account local conditions or contexts. Although assessments increasingly consider the demand for the ecosystem services that UGI provides, they tend to only map the spatial pattern of pressures such as heat, or air pollution, and lack a wider understanding of where the beneficiaries are located and who will benefit most. We assess UGI in five cities from four continents with contrasting climate, socio-political context, and size. For three example services (air pollution removal, heat mitigation, accessible greenspace), we run an assessment that takes into account spatial patterns in the socio-economic demand for ecosystem services and develops metrics that reflect local context, drawing on the principles of vulnerability assessment. Despite similar overall levels of UGI (from 35 to 50 % of urban footprint), the amount of service provided differs substantially between cities. Aggregate cooling ranged from 0.44 °C (Leicester) to 0.98 °C (Medellin), while pollution removal ranged from 488 kg $PM_{2.5}$/yr (Zomba) to 48,400 kg $PM_{2.5}$/yr (Dhaka). Percentage population with access to nearby greenspace ranged from 82% (Dhaka) to 100% (Zomba). The spatial patterns of pressure, of ecosystem service, and of maximum benefit within a city do not necessarily match, and this has implications for planning optimum locations for UGI in cities.

Keywords: Urban Green and Blue Space, Natural Capital, Ecosystem Services, Urban Planning, nature-based solutions (NBS).

Introduction

Approximately half of the world population currently live in cities, with this proportion projected to reach 60% by 2030 (Montgomery, 2007). As the urban fabric struggles to accommodate this influx, towns and cities expand and/or densify. By-products of these increases in urban population are increased air, water and noise pollution (e.g. from traffic, domestic waste and industry), increased anthropogenic heat outputs, as well as increased absorption of solar radiation and decreased emission of longwave energy (i.e. Urban Heat Island, UHI, effects - Mirzaei, 2015). With space at a premium, urban green and blue space, also termed urban green and blue infrastructure (UGI), typically makes way for man-made infrastructure, such as buildings and transport networks (e.g. through densification processes; Haaland et al., 2015). In turn, this reduction in UGI undermines the urban system's ability to regulate pressures such as heat, noise, air pollution and flooding (Foley et al., 2005; Derkzen et al., 2015), compounding the effects of urbanisation. Impacts of these pressures at an individual level often lead directly to poor health and declines in well-being.

The direct and indirect effects of these pressures on people are varied. $PM_{2.5}$ is the most damaging component of urban air pollution, with elevated $PM_{2.5}$ concentrations associated with negative health impacts such as premature death, lung cancer, pulmonary inflammation, altered cardiac function, and acute stroke mortality (Hong et al., 2002; Pope et al., 2002; Pope et al., 2004). High temperatures can place significant stress on the human body, with extremes leading to heat syncope, cardiovascular stress, thermal exhaustion or heat stroke (Kleerekoper et al., 2012). The severity of these conditions range from discomfort, impairment of physical and cognitive functions, to increases in morbidity and mortality rates. High temperatures in urban areas, in combination with air pollution, can also lead to increased ground-level ozone, which can have an antagonistic effect on cardio-respiratory conditions

(WHO, 2004). Increased incidence of psychosis and clinical depression, and decreased life satisfaction have all been connected to high levels of urbanisation, high population density and low levels of local-area urban green space (Sundquist et al., 2004; Chen et al., 2015; Cox et al., 2018; Houlden et al., 2018).

The United Nations Sustainable Development Goals (SDGs) include an emphasis on the importance of inclusive, accessible, multi-functional green spaces in urban settings, to provide a variety of benefits, including health and well-being to residents, especially target 11.7 of the UN Sustainable Development Goals (UN, 2017). UGI can have a significant cooling effect (Bowler et al., 2010a; Manteghi et al., 2015; Reis & Lopes, 2019), and vegetation removes particulate matter from the air column (Bealey et al., 2007; Chen et al., 2019). Exercise, or other physical activity in green or natural surroundings provides both short-term and long-term positive health outcomes (Barton & Pretty, 2010) and a number of studies have found links between availability of green spaces, the amount of exercise people take and physical health (e.g. Japan - Takano et al., 2002; Canada – Villeneuve et al., 2012). Many recent studies have identified associations between mental well-being and access/proximity to green space (e.g. Houlden et al. 2019). However, access to UGI, and the associated benefits, are often influenced by socio-economic status (e.g. Jenerette et al. 2011; Rutt & Gulsrud, 2016).

People in lower income neighbourhoods are typically at higher risk of exposure to, and lack the means to respond or adapt to, a number of these urbanisation-related pressures (Rosenthal, 2010; Pearce, 2013; Macintyre et al., 2018). For example, Neidell (2004) observed both greater exposure and greater effects of air pollution on asthmatic children of lower socio-economic status (SES) in California, USA (the authors cite affordability of living in areas with cleaner air as an impediment to lower SES families responding to/avoiding higher exposure). Children are particularly vulnerable and their exposure to these pressures can result in life-long impacts (Salthammer et al., 2016), not only in terms of health and well-being (Gauderman et al., 2005; McConnell et al., 2010), but also in terms of socio-economic mobility (Wargocki & Wyon, 2007). Additionally, differences in all-cause or selected-cause mortality have not been shown to be associated with extent of green space at the city-scale e.g. in the US (Richardson et al., 2012) and England (Bixby et al., 2015). This is critical because it suggests risks/benefits are highly localised, with likely implications for health inequalities. These concepts are fundamental to the emerging understanding of environmental justice in an urban context (Langemeyer & Connolly, 2020).

To date, studies of the ecosystem services (ES) provided by UGI in relation to health and well-being are typically focussed on low to medium population density, wealthy countries in North America, Europe and Asia, with relatively few in what is commonly referred to as the "Global South" (see Dados & Connell, 2012), i.e., predominantly low-income countries of South America, the Middle East and Africa (Gupta et al. 2016; Cruz-Garcia et al., 2017). As these low-income countries are predicted to be at the centre of projected future growth and urbanisation (Szabo, 2018), they should be the focus of research tackling the negative impacts of urbanisation and the associated inequality issues.

The majority of studies which attempt to map demand for ecosystem services pick easy metrics, which focus almost exclusively on mapping the pressure (Baró et al. 2015; Luederitz et al. 2015). They fail to take account of the location of the beneficiaries, and which beneficiaries are likely to benefit the most from service provision. An assessment which aims to tackle inequity issues needs to map and assess those sectors of the population who will benefit most from the ecosystem services that UGI provides, in combination with where the pressures are greatest and where the maximum ecosystem service can be delivered. These three dimensions are unlikely to be maximised in the same place.

In this study, we look at five cities across the world with a diversity of geographical, socio-political, climatic and economic contexts. Since there are relatively few Urban ES assessments in the Global South, we focus our assessments on four cities in this region, with a single city in the UK, Europe, for contrast (using the same methods). The aims of this study were firstly to demonstrate, using freely available open data sources, a means to identify and map urban green and blue space within a functional definition of urban footprint. We hypothesised that there would be variation in the congruence between the urban footprints and the administrational boundaries of the cities. Using the urban footprint as the basis of spatial analysis, and drawing on the principles of vulnerability assessment, we then aimed to answer the following questions: i) how do ES supply and socio-economic demand vary spatially within the study cities? and ii) what are the implications for calculating the health-related benefits from UGI in a way that is context-dependent? We select three important ecosystem services to illustrate this demand-focused approach: air pollution removal by woodland, heat mitigation, and accessible greenspace as a proxy for physical and mental wellbeing benefits. These represent important services in an urban context, with strong links to human health, especially in a global context (WHO 2018). Lastly, we compare and draw out commonalities across the cities. We hypothesised that the quantities of services provided would not be a simple function of extent/quantity of UGI; spatial context also being a factor. Further, we predicted that the highest demand for mitigation would not always be at locations where the pressures are greatest.

Methods:

The five case study cities are shown in Fig. 1: Dhaka City is a mega-city in Bangladesh, on the Ganges river delta, with population of 19,578,000, and extensive low-lying land with a relatively large area of water bodies. The two cities in Africa are somewhat smaller; Kigali in Rwanda has population of 1,058,000 and Zomba in Malawi a population of 105,000. Medellin is a relatively high altitude city in Colombia, with a population of 3,934,000 and very little blue space. Lastly, Leicester in the UK has a population of 354,000 and is part of a larger conurbation of urban areas in East Midlands of England. The cities are described in more detail in Appendix I.

[Fig. 1 here]

Land cover classification

We used a number of Spectral Indices as the basis for an enhanced land cover classification to identify urban green and blue space: Normalised Difference Vegetation Index (NDVI), Normalised Difference Built-up Index (NDBI), Normalised Difference Water Index (NDWI) and Urban Index (UI). These indices were calculated from cloud-free Sentinel-2a data (see table S1, in Supplementary Material for details) at a spatial resolution of ≈10 m (resampling to 10m, where necessary). Whilst NDVI alone is not always a good discriminant of different vegetation types, e.g. trees and grass, other spectral indices can be (e.g. NDWI, Szabo et al., 2016), and when multiple indices are combined, broad land cover classes, such as built up land, roads, grass and trees can be isolated (Duan et al., 2019).

We used unsupervised k-means clustering (kmc) to classify land cover into 10 classes, which were then assigned to one of four broad categories of urban land cover (after Jones et al., 2019), 'Built environment', 'High green' (woody, intensive vegetation, i.e. woodland), 'Low green' (non-woody, extensive vegetation, i.e. grass), 'Blue space' (water), using the True Colour Image (Sentinel-2a, TCI) for reference. Road networks and water bodies, including rivers, were extracted from Open Street Map (OSM), then used to update the classified raster dataset, in case any of these features were not detected in the satellite data.

Urban Footprint

Accurate urban extents are difficult to derive from administrative definitions (Balk et al., 2004). Many studies relating to urban ES use administrative boundaries to delimit the study area. However, these types of boundaries are of limited suitability for the purpose of assessing urban green and blue space. They are often not representative of the shape or size of the actual urbanised area, and they typically include large areas of woodland, grassland or cropland, which lie outside the urban area and are not part of the urban fabric. To undertake an objective quantitative assessment of urban green and blue space, we used a data-driven approach, based on the morphology of the urban fabric to define the urban footprint of our five case study cities.

We first used 'focal statistics', calculating a mean value within a (100 m x 100 m) neighbourhood region, applied to the 'Built environment' land cover class. We reclassified values of 0.15 and above as Urban. These urban areas were converted from raster into vector data - this threshold was chosen after sensitivity testing, using the TCI band as a reference. In order to identify and 'capture' green and blue space lying within the urban footprint we applied the variable positive-buffer and negative-buffer technique of Jones et al. (2019), to simplify the geometry of these polygons, selecting only polygons with an area greater than 1 km^2 and retaining only the geometry defining the overall perimeter of each polygon. The resulting urban footprint included all areas of green and blue space within the urban morphology and was used as the study extent for all further analyses.

Area calculations of land cover classes

Areas (km^2) of our land cover classes were calculated using polygon representations of the raster land cover dataset. Road networks, extracted from OSM, were used as an erase feature in order to delimit land cover parcels prior to the area calculations of green and blue space. We also created a combined 'Green space' category to aid interpretation, by merging the two vegetation classes using the dissolve function.

Data on pressures

In this study, we looked at two key urbanisation-related pressures (heat pressure and $PM_{2.5}$ pollution), with major health impacts (Jayasooriya et al. 2017; WHO 2018) using the following data: To estimate land surface temperature, we used Landsat satellite observations downloaded from USGS hub (https://earthexplorer.usgs.gov/). We used Landsat 8 OLI/TIRS

C1 L1 data and selected only imagery that had less than 10% cloud coverage. We analysed an 8-day composite from the hottest month of the year (2018) in Google Earth Engine (GEE) platform. First, we resampled all spectral bands into 30 m resolution, then, calculated land surface temperature after Sobrino, et al. (2004):

$$LST\ (°C) = \frac{\text{ABT}}{1 + (\lambda + T/\rho) ln\varepsilon} \qquad (1)$$

Where ABT is the atmosphere brightness temperature, λ is a wavelength and ρ =hc/k (1.438 x 10^{-2}mk), where h is Planck's constant (6.626 x 10^{-34}J/S), c is a velocity of light, k is Boltzman's constant (1.38x10^{-23} J/K), and ε is a surface emissivity ($\varepsilon = 0.004 * Pv + 0.989$) - in which Pv is the proportion of vegetation derived from maximum and minimum NDVI values.

For $PM_{2.5}$ we used the most up-to-date global dataset available at a suitably high resolution, 2016 $PM_{2.5}$ concentrations from MODIS, MISR and SeaWiFS Aerosol Optical Depth (AOD) with GWR (van Donkelaar et al., 2018).

Socio-economic data

The gridded population data for all five cities (people per pixel) are produced using a dasymetric modelling approach, using a Random Forest estimation technique to redistribute population count data, described in Stevens et al. (2015). Data for 2015 were used for all cities, except Leicester (2011). The data for Leicester was at a spatial resolution of 10 m, wheras data for other cities were at approximately 100 m (3 arc-seconds).

The gridded poverty data for Dhaka and Zomba (30 arc-second resolution) are created using Bayesian model-based geo-statistics in combination with high resolution gridded spatial covariates, applied to 2011 geo-located household survey data (Demographic and Health Survey, and Living Standards Measurement Study, respectively). The poverty indicator metric for Dhaka is likelihood of living in poverty (less than $2.50 per day) and the indicator for Zomba is the proportion of residents living in poverty (less than $2 per day). Poverty data for the other three cities were not available in gridded format, so figures are given at city district level (lower layer super output area, in the case of Leicester). The poverty indicator data for Kigali is the proportion of the population in poverty (less than 159,375 RWF per year), in 20013-14. For Medellin, the data are mean monthly income (2018), per city district. The income data were rescaled from zero to one and then inverted (i.e. 1 minus rescaled data), to represent prevalence of poverty. For Leicester, the poverty indicator used is the Index of Multiple Deprivation.

Quantification of Ecosystem Services (ES) provided by urban green and blue space

Air pollution removed ($PM_{2.5}$) by UGI was calculated using methods derived by re-analysis of data from Jones et al. (2017; 2019). A meta-model was created in the form of two regression equations to calculate quantity of $PM_{2.5}$ pollution removed by woodland, and the resulting change in $PM_{2.5}$ concentration. For the first equation, analysis showed that pollution removal was linearly related to amount of woodland, but efficiency varied according to $PM_{2.5}$ concentration. Therefore, we simplified the response variable to pollution removed per hectare of woodland, resulting in the following equation in which $PM_{2.5}$ concentration is the only predictor variable. This calculation can be used to calculate $PM_{2.5}$ removal rate of any sized area of woodland:

$$PM\_removal\_rate = 1.1664 * PM\_conc + 0.4837 \quad (2)$$

Where *PM_removal_rate* is quantity of $PM_{2.5}$ removed per unit area of woodland per year (kg ha^{-1} yr^{-1}), and *PM_conc* is the concentration of $PM_{2.5}$ ($\mu g\ m^{-3}$)

The second equation calculates the change in $PM_{2.5}$ concentration that occurs as a result of pollution removal through dry deposition processes, and is a function of the proportion of woodland in an area, the initial concentration of $PM_{2.5}$, and an interaction term between those two factors. Since a realistic change in pollutant concentration can only be achieved with vegetation over a large area, this equation is designed to be used at a city scale using average

PM concentration and overall proportion of woodland. Taking account of spatial location of beneficiaries and pollutant exposure within a city could be achieved by calculating a population-weighted average $PM_{2.5}$ concentration as an input to the equation. In this example, we used a city average $PM_{2.5}$ concentration, and percentage of woodland across each city.

$$Change\_PM\_conc = - 0.0318 * PM\_conc - 0.1112 * Log10WoodPC - 0.054 * PMxLogWood + 0.0832 \quad (3)$$

Where *Change_PM_conc* is the change in $PM_{2.5}$ concentration (μg m^{-3}), *PM_conc* is the initial $PM_{2.5}$ concentration (μg m^{-3}), *Log10WoodPC* is the Log10 of the percentage of woodland (percentage +1%, to avoid very low values) in the relevant area, and *PMxLogWood* is PM_conc multiplied by Log10WoodPC.

We used our "high green" land cover classification to represent woodland, and $PM_{2.5}$ concentrations (spatial mean within the urban footprint) were taken from the global dataset (van Donkelaar et al., 2018), with a spatial resolution of 0.01 decimal degrees (approx. 1 km at the equator).

Cooling effects were estimated by applying the methods of eftec et al. (2017), calculating relative coverage of each land cover type, multiplying by the respective land cover cooling coefficients and then summing all three values. We adjusted our cooling coefficients for high green land cover, proportionately, to mirror the climate effects observed by Morakinyo et al. (2017), assigning Dhaka and Zomba as 'hot humid' climate type, Kigali and Medellin as 'warm humid' climate type, and Leicester as 'temperate' climate type.

Due to the growing body of evidence supporting the positive relationship between access to green space and physical and mental health and well-being (H&W), we used 'access to green space' as a surrogate measure for the H&W benefit of urban green space. A number of metrics are used to quantify access to public spaces (e.g. Natural England, 2010; Wolch et al., 2011; Dadvand et al., 2012; Amoly et al., 2014; Bertram & Rehdanz, 2015; WHO, 2016). We used the indicator adopted by WHO which quantifies the population within a defined region living within 300 m radius (straight-line distance) of an open space of minimum size 0.5 ha (WHO, 2016). In our study, we applied a 300 m buffer to merged green space polygons with final minimum areas of ≥0.5 ha, counting the number of people within that buffer. Population data was derived from population distribution grids (see table S2 in Supplementary Material for details).

Mapping weighted demand, reflecting socio-economic context

The conceptual approach for calculating demand is shown in Fig. 2 and represents the principles that: more people equals greater impact, higher prevalence of poverty equals greater impact, and higher pressure equals greater impact. This draws on Vulnerability assessment, where the population (number of people in an area) is equivalent to exposure, and social factors such as poverty or age bracket represent sensitivity. Adaptive capacity is not represented in this context since that should cover both social and environmental adaptation. Therefore, weighted demand was calculated by multiplying rescaled population and poverty data by the rescaled pressure data, to give an equally-weighted output. In the scaling procedure, $PM_{2.5}$ and heat pressure data were rescaled (i.e. values of 0-1, based on min and max values in raw data within the urban footprint). The same procedure was applied to population and the poverty data (or equivalent indicator - see table S2). As there were no suitable pressure datasets for H&W, we combined the standardised population and prevalence of poverty data to represent a weighted demand, on the basis that higher prevalence of poverty is associated with lower health and well-being.

[Fig.2 here]

Mapping of ES supply

ES supply was calculated, e.g. the amount of pollution removed, the cooling provided using the methods described above, and based on the location of the relevant UGI (i.e. that which is providing the service). Focal statistics were used to characterise the area surrounding each raster cell to identify areas potentially benefitting from each service. For $PM_{2.5}$ removal, we applied a neighbourhood of 500m radius, based on other PM air pollution-related studies (e.g. Lei et al., 2018; Vivanco-Hidalgo et al., 2018; Wu et al., 2018; Chen et al., 2019). For cooling, supply was calculated as a proportion of the maximum possible (i.e. 100% high green cover) within a neighbourhood of radius 500 m (for consistency with PM removal). A number of the health and well-being benefits of green space involve being physically located at, or near to, the green spaces in question. For consistency with the WHO definition for accessible greenspace, we quantified the proportion of green land cover within a circular neighbourhood of radius 300 m.

Results

Urban footprints

For all cities, the derived urban footprint based on urban morphology is substantially smaller than the administrative boundary (Table 1 and Fig. 3). Large areas of green space surrounding the built-up 'urban' core of the cities (mainly comprising farmland, forest and scrub) are excluded from the analysis, which is focussed on **urban** green and blue spaces. It is also worth noting that the area of non-urban greenspace beyond the urban footprint varies considerably between cities, with the urban footprint occupying between 21% for Kigali and 98% for Leicester. Most of the urban footprints have multiple parts (a maximum of seven - Kigali), representing the sometimes discontinuous nature of the urban fabric within the administrative boundaries.

[Table 1 and Fig. 3 here]

Relative proportions of land covers

Despite the large variation in the size (Table 1) and historical development (Appendix I and Supplementary Material) of the five case study cities, there is relatively little variation in the proportional coverage of combined green and blue space (~15% variation). Most of the cities have very small proportions of blue space, although Dhaka with 5% has substantially more than the others. The two African cities, Kigali and Zomba, maintain noticeably more low green space than the other cities (between 12% and 15% more than the next highest). Most striking is the considerably higher proportion of high green coverage in Medellin, which has 13% coverage by area (a full 10% more than the next highest), despite having the lowest combined green and blue space coverage (only 35%).

Urban Green and blue space benefits

Variation in the $PM_{2.5}$ removal figures are broadly in proportion to ambient atmospheric concentrations (Table 2), although noticeable deviations from this trend are observed in Medellin and Zomba, due to their respectively higher and lower proportional urban woodland cover values – $PM_{2.5}$ removal being solely attributed to this class of land cover class.

[Table 2 here]

Mean estimated cooling effects of urban green and blue space (Table 2) are similar for Dhaka, Kigali and Zomba, when averaged across their entire urban footprint, with cooling effects between 0.6 °C and 0.65 °C. Leicester's urban green and blue space was estimated to provide a smaller cooling effect (0.44 °C) due to its temperate climate, in which urban woodland contributes less to the overall cooling effects. Medellin saw the largest cooling effect from urban green and blue space, of the five cities. This is because Medellin has a significantly higher proportion of the most effective land cover class for cooling (high green) relative to the other cities.

In terms of access to combined green space (i.e. high and low green aggregated, Fig. 4), all cities score highly, with a minimum of 84% of the urban footprint population (Dhaka) (Fig. 4b) and 92% of the total urban footprint (Dhaka and Medellin) (Fig. 4a) within 300 m of a parcel of green space at least 0.5 ha in area. When looking only at high green space, differences are more apparent. In Medellin, over 50% of the urban footprint population and 54% of the total urban footprint have access to high green, whereas the figure for the other cities lies between 17% and 25%.

[Fig. 4 here]

Overall, the differences in the proportion of combined green and blue space vary rather little between the five cities, by a maximum of a factor 1.5 (Table 1). However, the amount of service provided by this green and blue space shows much greater differences between cities. The largest difference is for pollution removal, where the estimated change in concentration due to vegetation differs by more than a factor of six between Zomba and Dhaka. The other two services, cooling by green and blue space, and access to greenspace differ by substantially lower amounts.

Spatial patterns in pressure, weighted demand, and ES supply

The spatial patterns of pressure, demand, and (potential) supply vary within cities and between different pressures within a city:

In Dhaka (Fig. 5), there is a strong gradient in $PM_{2.5}$ pressure, with the highest values in the North of the city diminishing in a Southerly direction. Heat pressure is more dispersed, with multiple focal points. For demand, there is an intense hotspot of demand for $PM_{2.5}$ removal in the far North of the city, while both H&W and cooling demand are greatest in a relatively small area in the south of the city. The supply of $PM_{2.5}$ removal is mainly concentrated in one area in the north-central region of the urban footprint. This region corresponds with the city airport, around which there are numerous trees. There are also a number of more intense pockets of supply in a general north-south band, through the centre of the city. Supply of cooling and of H&W mirrors the pattern of supply of $PM_{2.5}$ removal, but H&W values are typically higher.

In Kigali (Fig. S6), the high values of both $PM_{2.5}$ and heat pressures are greatest in the centre of the city, diminishing with distance outwards. Some of the smaller parts of the urban footprint also have elevated levels of these pressures, particularly those in the east. The demand for $PM_{2.5}$ removal, cooling and H&W are all highest around the western districts and are particularly intense around the nearby intersection of three major roads. Demand for all ES is lowest around the large green areas in the north of the urban footprint. The supply of $PM_{2.5}$ and cooling have similar distributions to one another, following the pattern of green space distribution seen in Fig. 3, with higher values around the north-central part of the main urban footprint. Supply of H&W benefits are particularly high in the same areas, but also in the Southern fringes of the main urban footprint, as well as the separate, smaller parts of the urban footprint.

In Leicester (Fig. S7), $PM_{2.5}$ and heat pressure distributions follow similar patterns, higher values in a north-south band following the centrally located river, extreme high values more common towards the northern and the southern ends. The demand for $PM_{2.5}$ and cooling share a similar distributional pattern, broadly following those of the pressures, but these are refined by the socio-economic data, creating dispersed pockets of intense demand. H&W demand follows the same pattern, although the pockets of high intensity demand do not diminish with distance from the central river. The supply of all three ES follow a consistent pattern but vary in degrees of intensity, with lowest levels of $PM_{2.5}$ removal supply, increasing up to a maximum with H&W supply. Higher values are distributed around the periphery of the urban footprint, with lower values dominating the city centre.

In Medellin (Fig. S8), the pressures of $PM_{2.5}$ and heat are both highest around the central transport artery (running from north to south), values diminishing with distance from this central line - more so to the east, where the terrain becomes steeper towards the edge of the urban footprint. Since high levels of $PM_{2.5}$ and heat pressure are fairly evenly distributed, the patterns of demand are more strongly influenced by the poverty data, which is recorded at district level and generally shows higher values in the west and the north of the city. $PM_{2.5}$ removal demand

and cooling demand are therefore highest in an outer band skirting the centre of the urban footprint. The distributional pattern of H&W demand follows the same pattern, but higher values are more prevalent. The supply of all three ES share a similar distributional pattern. Central areas typically show low levels of supply, with the exception of a centrally located park, whereas fringes of the urban footprint have higher values - particularly areas in the west of the city.

In Zomba (Fig. S9), $PM_{2.5}$ pressure is highest in the north of the city and diminishes in a south-easterly direction, whereas heat pressure is widespread, but with elevated values in the far west of the city, the south-east of the main part of the urban footprint and the far north east of the city. The demand for $PM_{2.5}$ removal and cooling is most intense in the far northeast of the urban footprint, around a major road. Demand for H&W follows the same pattern as demand for the other two ES, but with a general greater prevalence of higher values. The supply of $PM_{2.5}$ removal and cooling is largely confined to the western end of the eastern part of the urban footprint. This region comprises a relatively green university campus. The distribution of the supply of H&W is broadly the inverse of its demand, with lower values around the centre of the main urban footprint and the smaller eastern part.

As an overall comparison across cities, the amount and distribution of demand and service supply primarily reflect the combinations of intensity of the pressure, spatial patterns of demand, and the amount and type of UGI which is able to provide varying levels of ecosystem service to meet that demand. Each city has its own characteristics, and there is no consistent separation of the cities of the Global South from Leicester in the UK.

[Fig. 5 here]

Discussion

Urban Footprint

We chose to focus on *urban* green and blue infrastructure, rather than *all* green and blue infrastructure within an administrative region, so it was necessary to define the urban footprint based on the built environment. The difference in area of the administrative boundaries and their respective urban footprint highlights the importance of defining UGI in an objective way. The observed range just within these five cities, from 21% - 98% coverage of urban footprint within the administrative area, suggests that comparisons which only use administrative area may greatly over-estimate the amount of effective urban greenspace for many cities. This approach focusing on urban footprint is consistent with the definition of urban used for calculation of Sustainable Development Goal indicators for urban areas, e.g. SDG 11.7.1 on accessible open space (UN, 2015).

In this study, the administrative boundary was used to clip the continuous urban footprint for some cities in order to make best use of associated socio-economic data. Where other urban areas lie immediately adjacent to the boundary itself, or are continuous beyond that boundary, this may have two effects related to use and potential supply of ecosystem services lying either side of the boundary. Firstly, other UGI outside the boundary may benefit some of the population within the study area, while conversely UGI within the study area may provide additional benefit to adjacent urban areas. This provides a justification for a joined-up consultative approach to city planning, particularly where boundaries are strategically important, otherwise the risk is that fringe areas 'fall through the gaps' and are not appropriately considered in plans.

Ecosystem service supply

Although the overall proportion of combined UGI varied relatively little between our study cities, the amount of service that these areas provided showed larger differences. This illustrates primarily that UGI does not provide the same amount of service in every location, and therefore a context-specific analysis is required when assessing the benefits that it provides, not just a simple look-up table that is applied without discretion in all locations, which is unfortunately applied rather frequently (Campagne et al. 2020). This analysis shows that a context-specific analysis is possible with globally available datasets. For the pollution removal, this is partly because trees become more efficient at removing pollution when concentrations are higher (Nemitz et al. 2020), but the spatial context to the analysis plays a role in all three services in determining the level of benefit that can be attained.

Weighted demand

Our weighted demand metric provides a more useful and tractable representation of demand for mitigation than simplistic depictions of pressures (e.g. $PM_{2.5}$ concentrations) as it incorporates the human element, both in terms of exposure (i.e. number of people) and sensitivity (i.e. poverty). Similar approaches are now being applied in some cities, for example to inform performance planning of UGI to meet pre-specified objectives (Cortinovis & Geneletti 2020). Our results highlight that demand for different green intervention types can have different, and sometimes overlapping, spatial distributions. Differential spatial accessibility of greenspace has been shown in some studies, e.g. in Wuhan, China, accessibility to woods and parks differed in central city areas compared with the outskirts (He et al. 2020). Characterising the spatial pattern of demand is critical for addressing issues of inequity of access to UGI benefits, as the importance of environmental justice is increasingly recognised in urban planning (Wolch et al. 2014; Hunter et al. 2019; Langemeyer & Connolly 2020). As a result, it can help identify optimal locations for interventions, allowing decision makers to prioritise and obtain more effective outcomes, within a context of competing demands for budgets. It also allows effective design of interventions and management of trade-offs. For instance, trees are routinely planted to provide shade, to mitigate against urban heat problems, and to remove air pollution. However some tree species (e.g. eucalyptus) produce large quantities of Biogenic Volatile Organic Compounds (BVOCs), including isoprene, which can enhance the formation of secondary air pollutants, including PM and ozone (Yang et al., 2015).

Dhaka authority have previously planted Eucalyptus species for shading purposes (Ali, 1996). If they were to plant these trees in the north of the city, where there is elevated demand for both PM removal and cooling (see Fig. 5, panels A and E), the high output of BVOCs could potentially exacerbate the $PM_{2.5}$ problems.

Differences across cities

Relatively few assessments have been run on cities in the Global South, so the comparison of service provision among cities and with a European city is instructive. Despite widely different levels of pressure (e.g. $PM_{2.5}$ concentrations varying by nearly an order of magnitude) overall levels of service provision and proportions of UGI are broadly similar among cities. This suggests that the capacity for UGI to provide a service may be limited, and their contribution to mitigate extreme levels of pressure can not be considered a sole solution. Nonetheless, large variations in wealth and the ability to control one's own living conditions may mean that UGI in poorer neighbourhoods can achieve much greater benefit than in richer neighbourhoods where residents can afford to implement technical solutions in their homes to counter urban pressures such as heat and air pollution (Adegun 2017; de Souza Silva et al. 2018).

Reflections on the study approach

In this study we used broad classes of UGI, however further disaggregation of vegetation types would allow more accurate estimates for services that are reliant on the structure or type of vegetation. For example, cooling is influenced by leaf area index and structure of vegetation, described as vegetation intensity in some studies (see Morakinyo et al., 2017). Fine resolution estimates of vegetation canopy (e.g. from LiDAR) would enable calculation of vegetation height and volume, which would be a major step towards providing the basis for such disaggregation. Taking into account different vegetation types through additional land cover classes would also help improve estimates of air pollution removal which differ between deciduous trees and evergreen trees (Jones et al. 2017).

We used Sentinel-2a data, with a horizontal resolution of 10m. Although this is relatively fine resolution, it is still likely to underrepresent tree cover, in particular where trees are sparsely distributed. The implication of this is that pollution removal, relying entirely on high green land cover, is under-estimated, but probably not cooling effects because this requires a minimum threshold area of woodland to be effective (Yu et al., 2020). Rooftop gardening has become popular in Dhaka city, with approximately 36% of rooftops used for gardening and vegetation cultivation (Uddin et al., 2016). This form of green space will also likely be underrepresented in the land cover map, as the continuous area of these types of vegetation are typically much smaller than 10 m by 10 m. Further work on detection ability of satellite-derived NDVI would be highly valuable.

The H&W benefits provided by green space, as a venue for various activities (e.g. physical exercise, social interactions, etc.), is depend to a large extent upon public access. Regardless of the spatial resolution of remotely sensed data, public accessibility cannot be detected (Andries et al. 2019), which means that estimates of H&W based solely on such data must rely on the broad assumption that all green space is publicly accessible. Such assumptions will rarely be valid, as areas where the supply of ES are highest are not necessarily accessible. For instance, in Dhaka, the main hotspot for the supply of all our mapped ES (See Fig. 5 C, F & H), is a military restricted area that is not accessible to the general public. Other important factors, such as management and upkeep of these spaces, as well as the presence of amenities (e.g. cafes, public toilets, water fountains, etc.) are important factors in determining some components of useability (Wendel et al., 2012). Open spatial data identifying publicly accesible areas would be a valuable resource for quantifying the benefits of public UGI, as well as having the potential for increasing these benefits through informing the public of the availability of such venues. The supply and demand representation presented here could provide an effective focal point for local authority engagement by underscoring the multiple benefits of expanding accessabiity to these resources.

Use of global datasets allows consistent and objective comparisons of study cities, however they are typically the product of generalisation and may omit more localised, or fine-grain, patterns. For instance, the $PM_{2.5}$ dataset used in our study indicates that mean concentrations for Medellin are relatively low, at around 7 ug/m^3, however this is a substantial underestimate of concentrations experienced on the ground, which are nearer to 25 ug/m^3 (del Pilar et al., 2019). Air quality is often monitored at relatively few sites and may be subject to a number of sources of bias (e.g. monitoring stations only at locations of high concentration), which limit their utility in spatial analysis of supply and demand. Socio-economic datasets vary considerably between countries and cities in terms of which data are publicly available, at what spatial or administrative resolution, and how up-to-date the datasets are. Of these datasets, simple population data is arguably the most important, where it is available at census levels below that of entire city. This is because benefits are experienced by people. Beyond simple population, further breakdown according to socio-economic groups or proxy measures of wealth or deprivation, and breakdown according to age groups, both serve as ways to further differentiate risk among population to different groups. These risks may be different for particular pressures. For example age is an important risk factor for heat impacts (e.g. Gasparrini et al., 2012), and deprivation is important for air pollution (e.g. Cesaroni et al., 2013).

Conclusions

The approach outlined here, which focuses on urban footprint, avoids the inconsistencies which can arise from using administrative boundaries that include large areas of non-urban land cover. The approach also takes into account the location of green and blue space, and the exposure and vulnerability of the population to pressures associated with urbanisation. Together, this enables more accurate assessments of UGI, providing better information to planners and policy-makers. In relation to equity and environmental justice issues, this specifically allows planners to identify opportunities to redress socio-economic inequities, which might otherwise be missed – or worse, exacerbated. Thus, the approach outlined here can help prioritise interventions to improve both health and well-being, and the natural environment, by understanding the spatial relationships between service supply and demand.

Whilst the methods described here represent a useful development, further improvements in land cover classifications and data availability (particularly around public accessibility of land and socio-economic indicators) would improve the quality of information that can be provided to planners and policy-makers through this kind of analysis.

Acknowledgements

This work was supported by the University of Leicester’s QR Global Challenges Research Fund allocation (Research England); UK Natural Environment Research Council (grant no. NE/N005406/1 for Joshua D. Vande Hey).

Appendix

I: Case study city summaries:

Dhaka (population 19,578,000 – UN, 2018). The capital and largest city of Bangladesh, Dhaka is one of the largest and most densely populated cities in the world. It has a tropical, hot, humid climate and is located on the flat, low-lying, lower reaches of the Ganges delta, making it particularly vulnerable to sea level rise and flooding. A mega-city, Dhaka has been inhabited since the first millennium. It is a city of global strategic importance, which has experienced rapid population growth since the 1970s; although growth has diminished in more recent years, it is still very high (37.7% 2019). This persistent growth is driving urbanisation and is reflected in the city’s continued spatial expansion (Roy et al., 2019).

Kigali (population 1,058,000 – UN, 2018). The capital and largest city of Rwanda, Kigali has recently grown beyond 1 million people (with city boundaries expanded). It has a tropical, warm, humid climate and is located in a hilly landscape sprawling across four ridges, separated from each other by large valleys. Rapid hydrologic responses from highly urbanised sub-catchments in the city, in combination with poor drainage infrastructure management and lack of flood management knowledge, make flooding a major issue. Urban development often gives rise to dramatic changes in urban land use, where natural green spaces are removed and replaced with impervious built-up surfaces. There are plans for further development (2040 masterplan) including skyscrapers, pedestrian walkways and green spaces.

Leicester (population 354,000 – ONS, 2017). The UK city of Leicester is the most populous municipality within the East Midlands region and the 11th most populous in England. It has a temperate climate and is centred on the banks of the River Soar on flat to gently rolling terrain. One of the oldest cities in England, with a history going back at least two millennia, Leicester is a city with a historically moderate rate of population growth that has increased somewhat in recent decades.

Medellin (population 3,934,000 – UN, 2018): Medellin is the second largest city in Colombia, after the capital, Bogota. It has a tropical, warm, humid climate and is located within a narrow valley at approx. 1,500 m.a.s.l (60 km long and 8 to 10 km in its wider part). With its surrounding area containing nine other cities, the metropolitan area is the second largest agglomeration of population and economy (nearly four million inhabitants), in Colombia. Medellin was nominated for 'most innovative city of the year' in 2012 and won the award in 2013. Much new development is both planned and ongoing.

Zomba (population 105,000 – NSO, 2018). Zomba was the capital of Malawi until 1974, when this status was transferred to Lilongwe. It has a tropical, hot, humid climate and is located along the banks of the Mulunguzi River at the foot of the Zomba Plateau, an escarpment that rises to some 1800m. Although relatively small, Zomba is steadily growing (1977 - 24k, 2018 - 105k) and is now the fourth largest in Malawi.

References

Adegun, O.B. (2017). Green infrastructure in relation to informal urban settlements. *Journal of Architecture and Urbanism*, 41(1), pp.22-33.

Ali, M. (1996). Status, aspects and environmental considerations of Eucalyptus planting in Bangladesh. RAP Publication (FAO). url: http://www.fao.org/3/AC772E/ac772e02.htm

Amoly, E., Dadvand, P., Forns, J., López-Vicente, M., Basagaña, X., Julvez, J., ... & Sunyer, J. (2014). Green and blue spaces and behavioral development in Barcelona schoolchildren: the BREATHE project. *Environmental health perspectives*, *122*(12), 1351-1358.

Andries, A., Morse, S., Murphy, R.J., Lynch, J. and Woolliams, E.R., 2019. Seeing Sustainability from Space: Using Earth Observation Data to Populate the UN Sustainable Development Goal Indicators. Sustainability, 11(18), p.5062.

Balk, D., Pozzi, F., Yetman, G., Nelson, A., Deichmann, U. (2004). What can we say about urban extents? Methodologies to improve global population estimates in urban and rural areas? Population association of America annual meeting, Boston, MA

Baró, F., Haase, D., Gómez-Baggethun, E., Frantzeskaki, N. (2015). Mismatches between ecosystem services supply and demand in urban areas: A quantitative assessment in five European cities. *Ecol. Indic*. 55, 146-158. doi:10.1016/j.ecolind.2015.03.013

Barton, J., & Pretty, J. (2010). What is the best dose of nature and green exercise for improving mental health? A multi-study analysis. *Environmental science & technology*, *44*(10), 3947-3955.

Bealey, W. J., McDonald, A. G., Nemitz, E., Donovan, R., Dragosits, U., Duffy, T. R., & Fowler, D. (2007). Estimating the reduction of urban PM10 concentrations by trees within an environmental information system for planners. *Journal of Environmental Management*, *85*(1), 44-58.

Bertram, C., & Rehdanz, K. (2015). The role of urban green space for human well-being. Ecological Economics, 120, 139-152.

Bixby, H., Hodgson, S., Fortunato, L., Hansell, A., & Fecht, D. (2015). Associations between green space and health in English cities: an ecological, cross-sectional study. PLoS One, *10*(3).

Bowler, D. E., Buyung-Ali, L., Knight, T. M., & Pullin, A. S. (2010a). Urban greening to cool towns and cities: A systematic review of the empirical evidence. *Landscape and urban planning*, *97*(3), 147-155.

Campagne, C.S., Roche, P., Müller, F. and Burkhard, B. (2020). Ten years of ecosystem services matrix: Review of a (r) evolution. *One Ecosystem* 5 (2020), 5, p.e51103.

Cesaroni, G., Badaloni, C., Gariazzo, C., Stafoggia, M., Sozzi, R., Davoli, M., & Forastiere, F. (2013). Long-term exposure to urban air pollution and mortality in a cohort of more than a million adults in Rome. *Environmental health perspectives*, **121**(3), 324-331.

Chen, J., Chen, S., & Landry, P. (2015). Urbanization and mental health in China: linking the 2010 population census with a cross-sectional survey. *International journal of environmental research and public health*, **12**(8), 9012-9024.

Chen, M., Dai, F., Yang, B., & Zhu, S. (2019). Effects of neighborhood green space on PM2. 5 mitigation: Evidence from five megacities in China. *Building and Environment*, *156*, 33-45.

Cortinovis, C. and Geneletti, D. (2020). A performance-based planning approach integrating supply and demand of urban ecosystem services. *Landscape and Urban Planning*, 201, p.103842.

Cox, D. T., Shanahan, D. F., Hudson, H. L., Fuller, R. A., & Gaston, K. J. (2018). The impact of urbanisation on nature dose and the implications for human health. *Landscape and urban planning*, *179*, 72-80.

Cruz-Garcia, G. S., Sachet, E., Blundo-Canto, G., Vanegas, M., & Quintero, M. (2017). To what extent have the links between ecosystem services and human well-being been researched in Africa, Asia, and Latin America?. *Ecosystem Services*, *25*, 201-212.

Dados, N., & Connell, R. (2012). The global south. Contexts, *11*(1), 12-13.

Dadvand, P., Sunyer, J., Basagana, X., Ballester, F., Lertxundi, A., Fernandez-Somoano, A., Estarlich, M., Garcia-Esteban, R., Mendez, M. A. & Nieuwenhuijsen, M. J. 2012. Surrounding greenness and pregnancy outcomes in four Spanish birth cohorts. *Environmental Health Perspectives*, 120, 1481-1487.

de Sousa Silva, C., Viegas, I., Panagopoulos, T. and Bell, S. (2018). Environmental justice in accessibility to green infrastructure in two European cities. *Land*, 7(4), p.134.

del Pilar Arroyave-Maya, M., Posada-Posada, M. I., Nowak, D. J., & Hoehn, R. E. (2019). Remoción de contaminantes atmosféricos por el bosque urbano en el valle de Aburrá. *Colombia Forestal, 22*(1), 5-16.

Derkzen, M. L., van Teeffelen, A. J., & Verburg, P. H. (2015). Quantifying urban ecosystem services based on high-resolution data of urban green space: an assessment for Rotterdam, the Netherlands. *Journal of Applied Ecology*, *52*(4), 1020-1032.

Duan, Q., Tan, M., Guo, Y., Wang, X., & Xin, L. (2019). Understanding the spatial distribution of urban forests in China using Sentinel-2 images with Google Earth Engine*. Forests*, *10*(9), 729.

eftec (2017). A study to scope and develop urban natural capital accounts for the UK – Final Report, for DEFRA, June 2017. Available from: randd.defra.gov.uk/Document.aspx?Document=14143_UrbanNC_Account_FinalReportAugust2017.pdf

Foley, J. A., DeFries, R., Asner, G. P., Barford, C., Bonan, G., Carpenter, S. R., ... & Helkowski, J. H. (2005). Global consequences of land use. *science*, *309*(5734), 570-574.

Gasparrini, A., Armstrong, B., Kovats, S., & Wilkinson, P. (2012). The effect of high temperatures on cause-specific mortality in England and Wales. *Occupational and environmental medicine*, **69**(1), 56-61.

Gauderman, W.J., Avol, E., Lurmann, F., Künzli, N., Gilliland, F., Peters, J. and McConnell, R. (2005) Childhood asthma and exposure to traffic and nitrogen dioxide, *Epidemiology*, **16**, 737–743.

Gupta, K., Roy, A., Luthra, K., & Maithani, S. (2016). GIS based analysis for assessing the accessibility at hierarchical levels of urban green spaces. *Urban forestry & urban greening*, *18*, 198-211.

Haaland, C., & van Den Bosch, C. K. (2015). Challenges and strategies for urban green-space planning in cities undergoing densification: A review. *Urban forestry & urban greening*, 14(4), 760-771.

He, S., Wu, Y. and Wang, L., 2020. Characterizing horizontal and vertical perspectives of spatial equity for various urban green spaces: a case study of Wuhan, China. Frontiers in Public Health, 8.

Hong, Y.C., Lee, J.T., Kim, H., Ha, E.H., Schwartz, J., Christiani, D.C., 2002. Effects of air pollutions on acute stroke mortality. Environmental Health Perspectives 110, 187e191

Houlden, V., Weich, S., de Albuquerque, J. P., Jarvis, S., & Rees, K. (2018). The relationship between greenspace and the mental well-being of adults: a systematic review. *PloS one*, *13*(9), e0203000.

Houlden, V., de Albuquerque, J. P., Weich, S., & Jarvis, S. (2019). A spatial analysis of proximate greenspace and mental well-being in London. Applied Geography, *109*, 102036.

Hunter, R.F., Cleary, A. and Braubach, M. (2019). Environmental, health and equity effects of urban green space interventions. In Biodiversity and Health in the Face of Climate Change (pp. 381-409). Springer, Cham.

Jayasooriya, V. M., Ng, A. W. M., Muthukumaran, S., & Perera, B. J. C. (2017). Green infrastructure practices for improvement of urban air quality. Urban Forestry & Urban Greening, 21, 34-47.

Jeanjean, A. P., Buccolieri, R., Eddy, J., Monks, P. S., & Leigh, R. J. (2017). Air quality affected by trees in real street canyons: The case of Marylebone neighbourhood in central London. Urban Forestry & Urban Greening, *22*, 41-53.

Jenerette, G. D., Harlan, S. L., Stefanov, W. L., & Martin, C. A. (2011). Ecosystem services and urban heat riskscape moderation: water, green spaces, and social inequality in Phoenix, USA. Ecological applications, *21*(7), 2637-2651.

Jones, L., Vieno, M., Morton, D., Cryle, P., Holland, M., Carnell, E., Nemitz, E., Hall, J., Beck, R., Reis, S., Pritchard, N., Hayes, F., Mills, G., Koshy, A., Dickie, I. (2017). Developing Estimates for the Valuation of Air Pollution Removal in Ecosystem Accounts. Final report for Office of National Statistics, July 2017.

Jones, L., Vieno, M., Fitch, A., Carnell, E., Steadman, C., Cryle, P., Holland, M., Nemitz, E., Morton, D., Hall, J. & Mills, G. (2019). Urban natural capital accounts: developing a novel approach to quantify air pollution removal by vegetation. *Journal of Environmental Economics and Policy*, *8*(4), 413-428 (URL: https://doi.org/10.1080/21606544.2019.1597772)

Kleerekoper, L., Van Esch, M., & Salcedo, T. B. (2012). How to make a city climate-proof, addressing the urban heat island effect. *Resources, Conservation and Recycling*, *64*, 30-38.

Langemeyer, J., Connolly, J.J.T. (2020). Weaving notions of justice into urban ecosystem services research and practice. *Environ. Sci. Policy* 109, 1-14. doi:10.1016/J.ENVSCI.2020.03.021

Lee, J. K., Acharya, T. D., & Lee, D. H. (2018). Exploring land cover classification accuracy of Landsat 8 image using spectral index layer stacking in hilly region of South Korea. *Sensors and Materials*, *30*(12), 2927-2941.

Lei, Y., Duan, Y., He, D., Zhang, X., Chen, L., Li, Y., ... & Zheng, J. (2018). Effects of urban greenspace patterns on particulate matter pollution in metropolitan Zhengzhou in Henan, China. *Atmosphere*, *9*(5), 199.

Luederitz, C., Brink, E., Gralla, F., Hermelingmeier, V., Meyer, M., Niven, L., Panzer, L., Partelow, S., Rau, A.-L., Sasaki, R., Abson, D.J., Lang, D.J., Wamsler, C., von Wehrden, H. (2015). A review of urban ecosystem services: six key challenges for future research. *Ecosyst. Serv*. 14, 98-112. doi:10.1016/j.ecoser.2015.05.001

Macintyre, H. L., Heaviside, C., Taylor, J., Picetti, R., Symonds, P., Cai, X. M., & Vardoulakis, S. (2018). Assessing urban population vulnerability and environmental risks across an urban area during heatwaves–Implications for health protection. Science of the total environment, 610, 678-690.

Manteghi, G., bin Limit, H., & Remaz, D. (2015). Water bodies an urban microclimate: A review. *Modern Applied Science*, *9*(6), 1.

McConnell, R., Islam, T., Shankardass, K., Jerrett, M., Lurmann, F., Gilliland, F., Gauderman, J., Avol, E., Künzli, N., Yao, L., Peters, J. and Berhane, K. (2010) Childhood incident asthma and traffic-related air pollution at home and school, *Environ. Health Perspect.*, **118**, 1021–1026.

Mirzaei, P. A. (2015). Recent challenges in modeling of urban heat island. *Sustainable cities and society*, *19*, 200-206.

Montgomery, M. (2007). United Nations Population Fund: State of world population 2007: Unleashing the potential of urban growth. *Population and Development Review*, *33*(3), 639-641.

Morakinyo, T. E., Dahanayake, K. K. C., Ng, E., & Chow, C. L. (2017). Temperature and cooling demand reduction by green-roof types in different climates and urban densities: A co-simulation parametric study. *Energy and Buildings*, *145*, 226-237.

Natural England. (2010). Nature nearby: accessible natural greenspace guidance. *Natural England: Peterborough*.

Neidell, M. J. (2004). Air pollution, health, and socio-economic status: the effect of outdoor air quality on childhood asthma. *Journal of health economics*, *23*(6), 1209-1236.

Nemitz, E., Vieno, M., Carnell, E., Fitch, A., Steadman, C., Cryle, P., Holland, M., Morton, R.D., Hall, J., Mills, G., Hayes, F., Dickie, I., Carruthers, D., Fowler, D., Reis, S., Jones, L. (2020). Potential and limitation of air pollution mitigation by vegetation and uncertainties of deposition-based evaluations. *Philosophical Transactions of the Royal Society A*, 378(2183), p.20190320.

NSO - National Statistics Office of Malawi (2018). 2018 Population and Housing Census, Preliminary report. URL: https://malawi.unfpa.org/sites/default/files/resource-pdf/2018%20Census%20Preliminary%20Report.pdf

ONS (2017) Population Estimates for England and Wales, Scotland and Northern Ireland: time-series. URL: https://www.ons.gov.uk/datasets/mid-year-pop-est/editions/time-series/versions/4

Pearce, J. (2013). An environmental justice framework for understanding neighbourhood inequalities in health and well-being. In *Neighbourhood Effects or Neighbourhood Based Problems?* (pp. 89-111). Springer, Dordrecht.

Pope, C.A., Burnett, R.T., Thun, M.J., Calle, E.E., Krewski, D., Ito, K., Thurston, G.D., 2002. Lung cancer, cardiopulmonary mortality, and long-term exposure to fine particulate air pollution. Journal of the American Medical Association 287 (9), 1132e1141.

Pope, C.A., Burnett, R.T., Thurston, G.D., Thun, M.J., Calle, E.E., Krewski, D., Godleski, J.J., 2004. Cardiovascular mortality and long-term exposure to particulate air pollution. Circulation 109, 71e77

Reis, C., & Lopes, A. (2019). Evaluating the Cooling Potential of Urban Green Spaces to Tackle Urban Climate Change in Lisbon. *Sustainability*, *11*(9), 2480.

Richardson, E. A., Mitchell, R., Hartig, T., De Vries, S., Astell-Burt, T., & Frumkin, H. (2012). Green cities and health: a question of scale?. J Epidemiol Community Health, *66*(2), 160-165.

Rosenthal, J. K. (2010). *Evaluating the impact of the urban heat island on public health: Spatial and social determinants of heat-related mortality in New York City* (Doctoral dissertation, Columbia University).

Roy, S., Sowgat, T., & Mondal, J. (2019). City Profile: Dhaka, Bangladesh. *Environment and Urbanization ASIA, 10*(2), 216-232.

Rutt, R. L., & Gulsrud, N. M. (2016). Green justice in the city: A new agenda for urban green space research in Europe. Urban forestry & urban greening, 19, 123-127.

Salthammer, T., Uhde, E., Schripp, T., Schieweck, A., Morawska, L., Mazaheri, M., ... & Viana, M. (2016). Children's well-being at schools: impact of climatic conditions and air pollution. *Environment international*, *94*, 196-210.

Sobrino, J. A., Jimenez-Munoz, J. C., & Paolini, L. (2004). Land surface temperature retrieval from LANDSAT TM 5. *Remote Sensing of environment*, *90*(4), 434-440.

Stevens F. R., Gaughan A, E., Linard C, Tatem A. J. (2015). Disaggregating Census Data for Population Mapping Using Random Forests with Remotely-Sensed and Ancillary Data. *PLoS ONE* 10(2): e0107042. https://doi.org/10.1371/journal.pone.0107042Sundquist, K., Frank, G., & Sundquist, J. A. N. (2004). Urbanisation and incidence of psychosis and depression: follow-up study of 4.4 million women and men in Sweden. *The British Journal of Psychiatry*, *184*(4), 293-298.

Szabo, C. P. (2018). Urbanization and mental health: a developing world perspective. *Current opinion in psychiatry*, *31*(3), 256-257.

Szabo, S., Gácsi, Z., & Balazs, B. (2016). Specific features of NDVI, NDWI and MNDWI as reflected in land cover categories. Landscape & Environment, *10*(3-4), 194-202.

Takano, T., Nakamura, K., & Watanabe, M. (2002). Urban residential environments and senior citizens’ longevity in megacity areas: the importance of walkable green spaces. *Journal of Epidemiology & Community Health*, *56*(12), 913-918.

Uddin, M. J., Khondaker, N. A., Das, A. K., Hossain, M. E., Masud, A. D. H., Chakma, A. S., ... & Chowdhury, A. A. (2016). *Baseline Study on Roof Top Gardening in Dhaka and Chittagong City of Bangladesh* (Vol. 8, p. 4). A final technical report under the project of “Enhancing Urban Horticulture Production to Improve Food and Nutrition Security” (TCP/BGD/3503) funded by Food and Agriculture Organization of the United Nations. FAO Representation in Bangladesh. Road.

UN (2015). Transforming our world: The 2030 Agenda for Sustainable Development. General Assembly 70 Session. 2015, 16301, 1–35.

UN. (2017). United Nations General Assembly. New Urban Agenda 2017. http://habitat3.org/the-new-urbanagenda.

UN. (2018). The world’s cities in 2018 – Data booklet. ISBN: 9210476107, 9789210476102

van Donkelaar, A., R. V. Martin, M. Brauer, N. C. Hsu, R. A. Kahn, R. C. Levy, A. Lyapustin, A. M. Sayer, and D. M. Winker. 2018. Global Annual PM2.5 Grids from MODIS, MISR and SeaWiFS Aerosol Optical Depth (AOD) with GWR, 1998-2016. Palisades NY: NASA Socioeconomic Data and Applications Center (SEDAC). https://doi.org/10.7927/H4ZK5DQS. Accessed 01/08/2019.

Villeneuve, P. J., Jerrett, M., Su, J. G., Burnett, R. T., Chen, H., Wheeler, A. J., & Goldberg, M. S. (2012). A cohort study relating urban green space with mortality in Ontario, Canada. *Environmental research*, *115*, 51-58.

Vivanco-Hidalgo, R. M., Wellenius, G. A., Basagaña, X., Cirach, M., González, A. G., de Ceballos, P., ... & Alastuey, A. (2018). Short-term exposure to traffic-related air pollution and ischemic stroke onset in Barcelona, Spain. *Environmental research, 162*, 160-165.

Wargocki, P., Wyon, D.P., 2007. The effects of moderately raised classroom temperatures and classroom ventilation rate on the performance of schoolwork by children (RP-1257). HVAC&R Res. 13, 193–220.

Wendel, H. E. W., Zarger, R. K., & Mihelcic, J. R. (2012). Accessibility and usability: Green space preferences, perceptions, and barriers in a rapidly urbanizing city in Latin America. *Landscape and urban planning*, *107*(3), 272-282.

WHO. 2004. In: Health and global environmental change; 2004.

WHO. 2016. *Urban green spaces and health.* Copenhagen: WHO Regional Office for Europe, 2016.

WHO. 2018. World health statistics 2018: monitoring health for the SDGs, sustainable development goals. Geneva: World Health Organization; 2018. Licence: CC BY-NC-SA 3.0 IGO. Available online https://apps.who.int/iris/handle/10665/272596 [Last accessed: 2021, January 10]

Wolch, J.R., Byrne, J. and Newell, J.P. (2014). Urban green space, public health, and environmental justice: The challenge of making cities ‘just green enough’. *Landscape and urban planning*, 125, pp.234-244.

Wolch, J., Jerrett, M., Reynolds, K., Mcconnell, R., Chang, R., Dahmann, N., Brady, K., Gilliland, F., Su, J. G. & Berhane, K. 2011. Childhood obesity and proximity to urban parks and recreational resources: A longitudinal cohort study. *Health & Place*, 17, 207-214.

Wu, H., Yang, C., Chen, J., Yang, S., Lu, T., & Lin, X. (2018). Effects of Green space landscape patterns on particulate matter in Zhejiang Province, China. *Atmospheric Pollution Research, 9*(5), 923-933.

Yu, Z., Yang, G., Zuo, S., Jørgensen, G., Koga, M., & Vejre, H. (2020). Critical review on the cooling effect of urban blue-green space: A threshold-size perspective. Urban Forestry & Urban Greening, 126630.Yang, J., Chang, Y., & Yan, P. (2015). Ranking the suitability of common urban tree species for controlling PM2. 5 pollution. Atmospheric pollution research, 6(2), 267-277.

Zhu, Y., Hinds, W. C., Kim, S., Shen, S., & Sioutas, C. (2002). Study of ultrafine particles near a major highway with heavy-duty diesel traffic. *Atmospheric environment*, *36*(27), 4323-4335.

Figure Legends

Figure 1. Locations of the five Case study cities. Images from Google Earth (31 March 2020).

Figure 2. Conceptual approach to deriving 'weighted demand' for ES. Higher numbers of people, higher levels of poverty and higher levels of pressure all lead to increased demand.

Figure 3. Land Cover maps for A) Dhaka City, B) Kigali City, C) Leicester City, D) Medellin City, E) Zomba City, and F) the true colour satellite imagery for Zomba City (for reference with 'E') showing the administrative boundary and the urban footprint.

Figure 4. Access to green spaces and to high green spaces, of minimum 0.5 ha, calculated as % of urban footprint (A), and % of population (B), within 300 m.

Figure 5. ***Dhaka –*** *Mapped pressures, ES supply and weighted demand. Panels depict: A) $PM_{2.5}$ pressure, B) $PM_{2.5}$ weighted demand, C) $PM_{2.5}$ removal service supply, D) Heat pressure, E) Cooling weighted demand, F) Cooling service supply, G) H&W weighted demand, H) H&W service supply.*

Figures

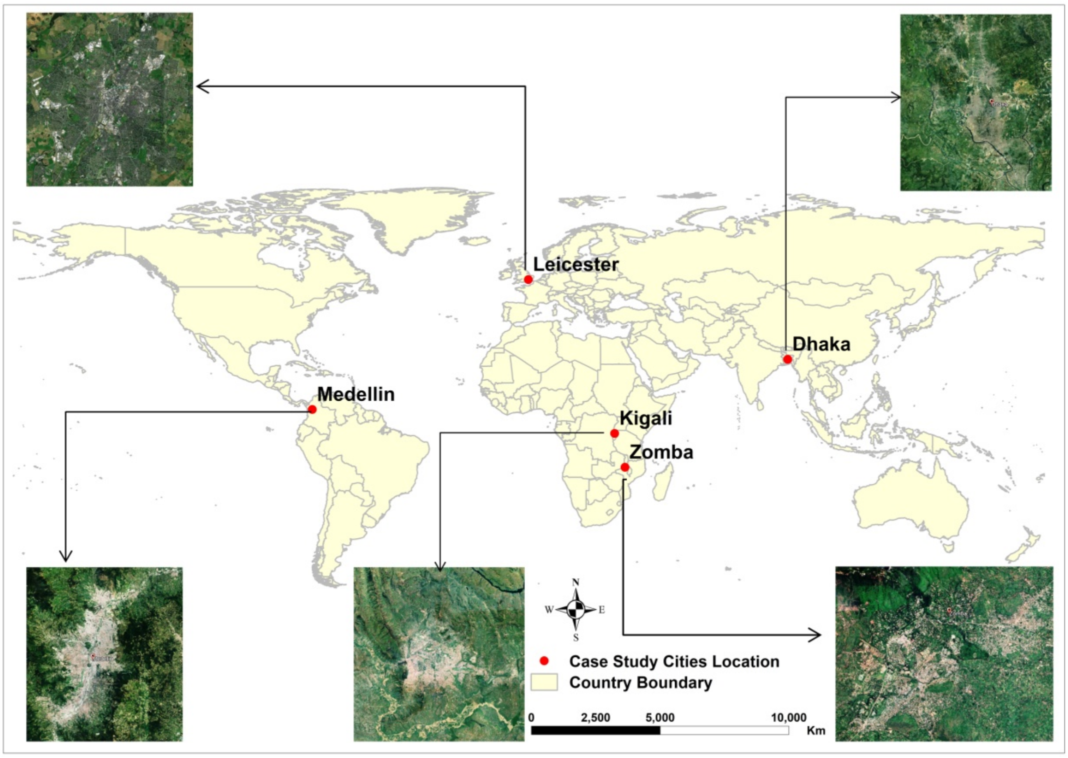

Figure 1.

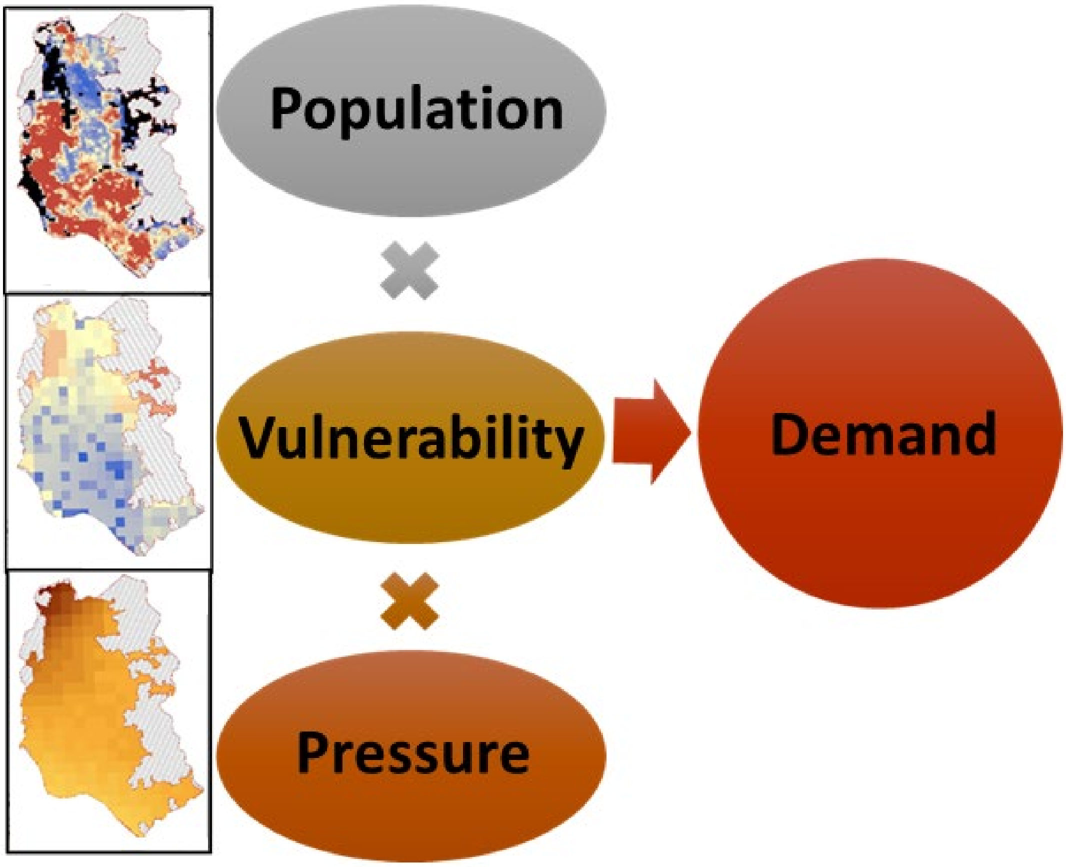

886 *Figure 2.*

887

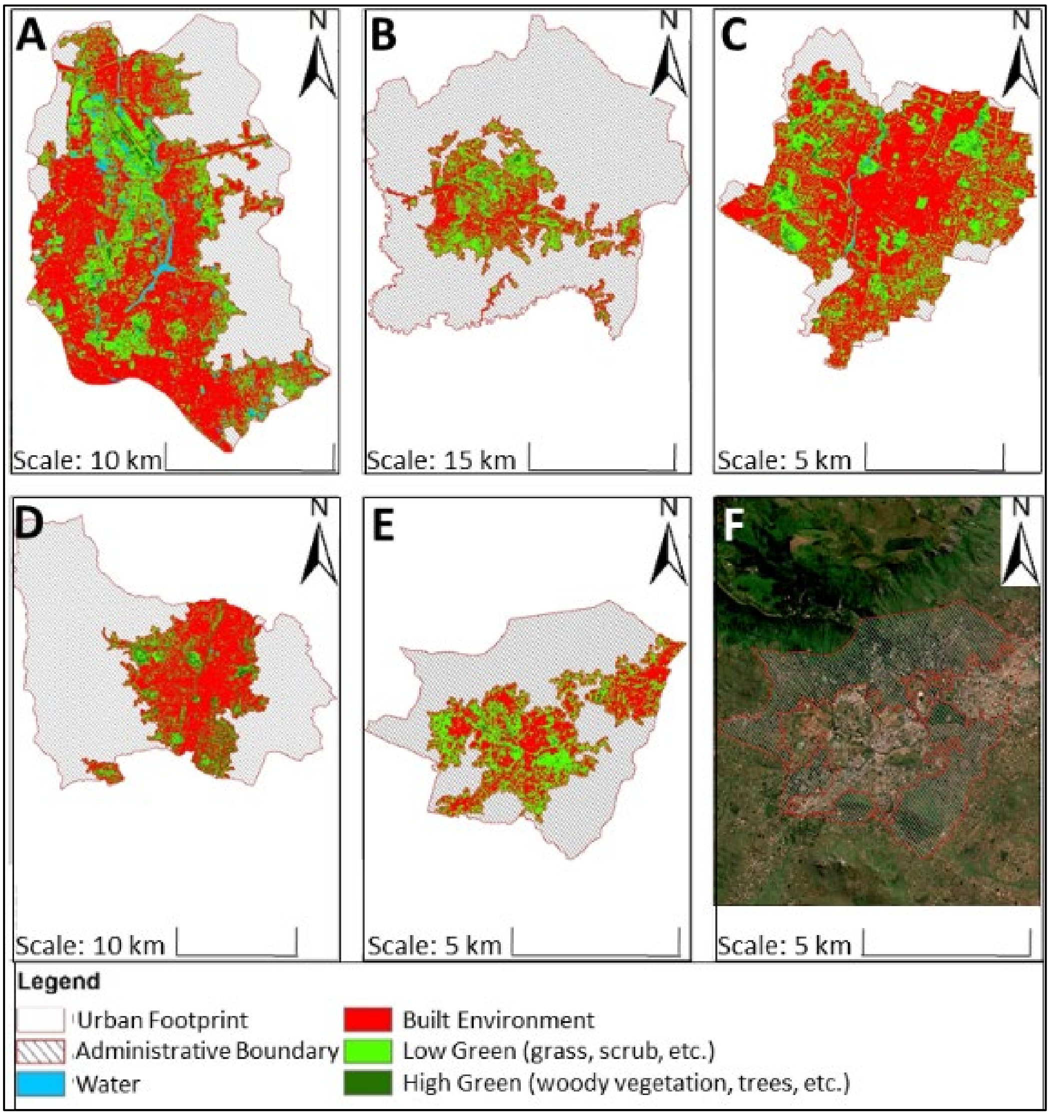

889 *Figure 3.*

890

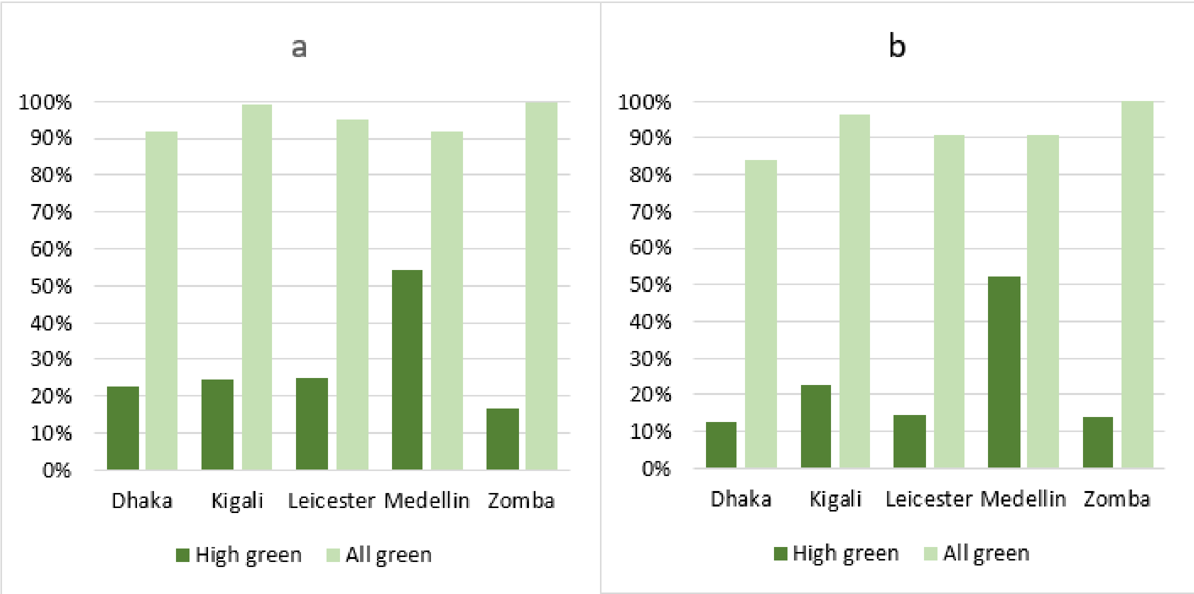

892 *Figure 4.*

893

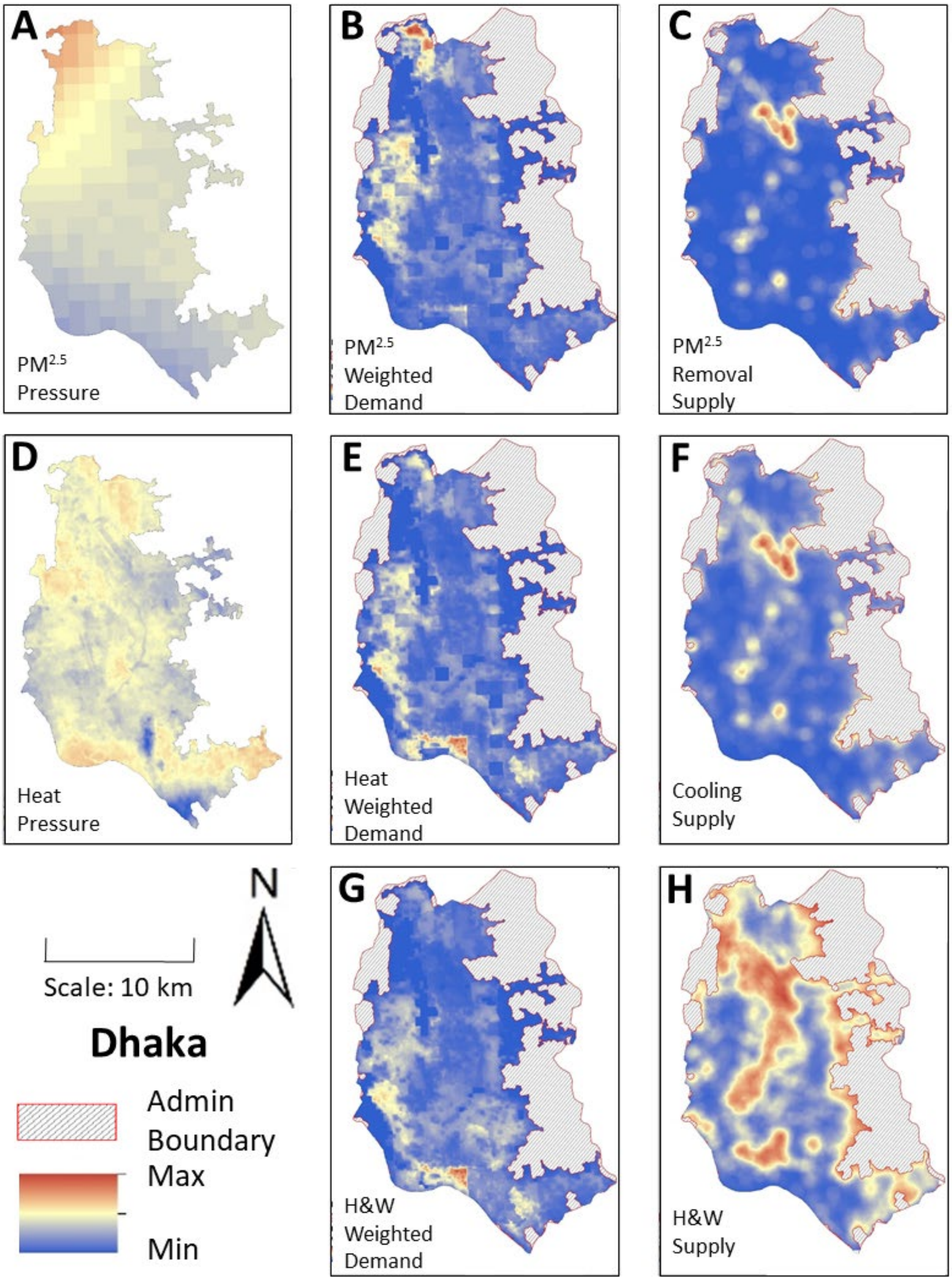

895 *Figure 5.*

896

897

898

Tables

Table *1. Urban footprint (UF) areas, the percentage they occupy of the administrative boundaries, and the % land cover types of the UF area, for each of the five cities.*

City	UF Area (km^2)	UF as % of Admin Area	High green	Low Green	Blue space	Combined Blue/green space
Dhaka	209.2	70.0%	3.1%	32.9%	4.52%	40.6%
Kigali	156.6	21.5%	2.5%	47.7%	0.13%	50.3%
Leicester	64.5	97.9%	3.5%	33.6%	0.52%	37.6%
Medellin	117.8	31.8%	13.1%	21.7%	0.06%	34.9%
Zomba	16.2	38.7%	2.4%	45.2%	0.03%	47.7%

Table 2. Ecosystem service values for $PM_{2.5}$ removal and cooling provided by urban green and blue space, for each of the five case study cities. Ambient $PM_{2.5}$ and maximum daily temperatures for 2018 also provided for information.

City	$PM_{2.5}$ removed by woodland (kg/yr)	Estimated change in $PM_{2.5}$ due to trees (μg/m^3)	Aggregate cooling effect (°C)	Ambient $PM_{2.5}$ (μg/m^3)	Max daily Temp (2018) (°C)
Dhaka	48,402	-4.12	-0.63	63.58	37
Kigali	11,368	-1.49	-0.6	24.73	30
Leicester	3,265	-0.83	-0.44	12.53	33
Medellin	13,164	-0.73	-0.98	7.3	31
Zomba	488	-0.62	-0.65	10.6	36